

Dynamic Contrast Enhanced MRI Post-Prostatectomy for a Rising PSA: Implications for Radiotherapy

R. Stoyanova¹, R. Rajpara¹, E. Bossart¹, V. Casillas², J. Palma¹, M. Abdel-Wahab¹, and A. Pollack¹

¹Radiation Oncology, University of Miami, Miami, Florida, United States, ²Diagnostic Radiology, University of Miami, Miami, Florida, United States

Introduction: The treatment of choice for biochemical failure and local recurrence (LR) of prostate cancer (PCa) after radical prostatectomy (RP) is salvage radiotherapy (RT). Identifying the treatment volumes for these patients is challenging¹. Dynamic Contrast Enhanced Magnetic Resonance Imaging (DCE-MRI) may be useful in identifying the location and extent of recurrent PCa. DCE-MRI has been shown to have greater sensitivity and specificity for PCa localization before RP² as compared to T2-weighted MRI (T2-w) alone. However, there are few imaging studies related to post-prostatectomy patients³. In this study, we used DCE-MRI to identify LR of PCa in men who underwent RP and had a subsequent rising Prostate-Specific Antigen (PSA).

Methods: The medical records of 15 patients referred for RT consultation at the University of Miami Sylvester Comprehensive Cancer Center from June 1, 2008 to September 1, 2009 were reviewed. The DCE-MRI data were obtained on a 3T MR scanner (Siemens Trio Tim, Erlangen, Germany): resolution 0.7 mm × 0.7 mm × 2.5 mm; field of view: 360 × 264 mm; 72 slices (no gap); 5.1 ms repetition time/2.3 ms echo time; flip angle 10°. Prior to contrast material injection, one set of MR images was acquired, followed by 11-12 post-contrast imaging datasets (37 s each). The DCE-MRI images were analyzed with software utilizing pattern recognition techniques for deconvolution of the contrast-to-time patterns. Briefly, Principal Component Analysis (PCA) is applied to detect the number of significant Principal Components (PCs). PCA also identifies sources of variations resulting from movement and other such artefacts⁴. The image series from time points with unwanted variations are removed from further analysis. Afterwards the data is analyzed with the constrained non-negative matrix factorization (cNMF)⁵ method which assumes each image represents a mixture of k tissue components. k is estimated from the number of significant PCs. A characteristic contrast-to-time curve is associated with each tissue component. cNMF determines the shape of the k basic curves and their weights, displayed as a heat map representing the location of the particular tissue subcomponent, related to its corresponding curve. A major advantage of the technique is that the identified curves have direct physical interpretation. We can visually inspect the temporal pattern of the contrast enhancement (fast, slow, constant) and relate the amplitude (weight) of the pattern to particular tissue. Specifically, tumors are detected by their characteristic temporal profile, defined by relatively fast contrast uptake and washout.

Results: The median age of the 15 patients presenting for RT was 62 years (43 – 71). Three (20%) patients had a Gleason Score (GS) of 6, five (33%) had a GS of 7, four (27%) had a GS of 8, and three (20%) had a GS of 9. The median pre-RT PSA was 0.5 (0.11 – 9.2). Ten (67%) patients had positive margins, two (13%) had seminal vesicle (SV) involvement, and seven (47%) had extracapsular

extension. The median time for presentation for RT after RP was 18 months (3 – 120). PCA was applied to the DCE-MRI dataset from each patient. Visual inspection of the PCs can be extremely informative about the number and types of variations present in the data. In Figure 1, for example, the first four PCs from analysis of a DCE-MRI dataset are shown. It is clear that while the first three PCs have a smooth character, the fourth has a spike at the 9th time-point of acquisition (marked with an arrow). Based on the corresponding score-image, it can be inferred that there was a sudden deformation of the rectum. Indeed, a close inspection of the image data from this slice at this time point indicates changes in the rectum shape. These “flawed” series were removed from further analysis. Further, the Region of Interest (ROI) was outlined and cNMF applied, seeking as many patterns as the number of significant PCs. In Figure 2 cNMF results from another patient are presented. The area of the tumor, corresponding to the characteristic tumor temporal pattern is depicted with a heat map on the T2-w. It is clear that in this case a significant volume in the base of the bladder is suspicious for malignancy. Overall eleven

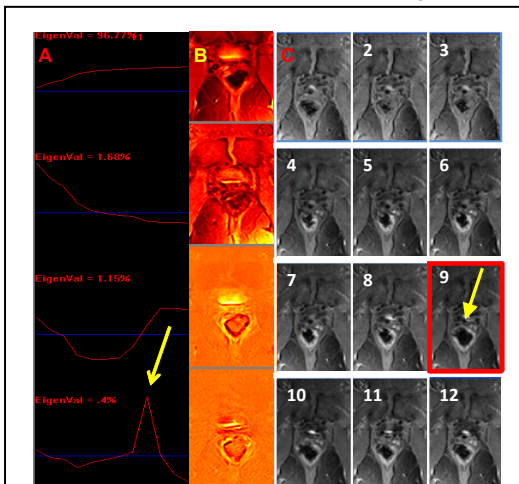


Figure 1. PCA analysis of DCE-MRI data of a post-prostatectomy patient. (A) First four PCs, together with the fraction of total variance they explain. In the 4th PC an arrow indicates an abrupt change in the 9th time-point of DCE acquisition; (B) Spatial distribution of the magnitude of the corresponding PCs scores; (C) Raw image data from the same axial slice over the course of the DCE-MRI data collection (12 time points). There is a change in the rectum shape (yellow arrow) in the 9th series (red box).

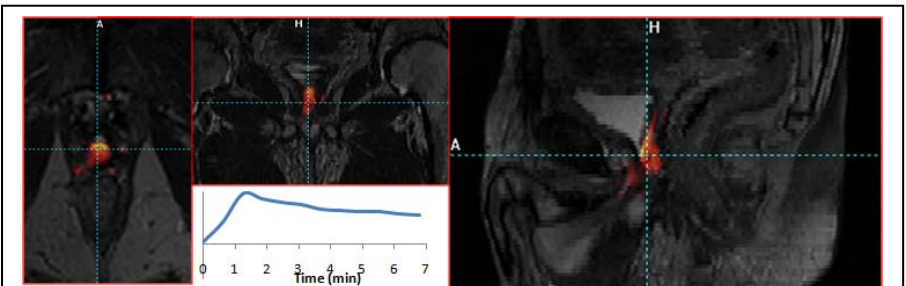


Figure 2. Analysis of DCE-MRI dataset from a patient post-prostatectomy. Axial, sagittal and coronal T2-w views overlaid with a color map depicting the area of the tumor. Insert: Temporal contrast uptake and washout pattern of the tumor.

(73.3%) patients had findings suggestive of tumor as visualized by DCE-MRI. Only four of these (36%) had a palpable abnormality on digital rectal examination prior to RT. A total of 17 areas suspicious for malignancy were identified: 10 in the prostate bed; 4 in lymph nodes; and 3 in the SV remnants.

Conclusions: Our data indicate that MRI, combined with DCE, detects abnormalities suggestive of residual tumor in the prostate bed in nearly 75% of patients evaluated for RT. Because patients treated with salvage RT often develop a rising PSA later and there is some evidence for a RT dose response, targeting of the contrast-enhancing areas specifically may improve tumor control and limit toxicity.

References: ¹Michalski JM, et al. *Int J Radiat Oncol Biol Phys* 2009. ²Padhani AR, et al. *Clin Radiol* 2000;55:99-109. ³Scattoni V, et al. *BJU Int* 2004;93:680-688. ⁴Stoyanova R, Brown TR. *J Magn Reson* 2002;154:163-175. ⁵Du S, Sajda P, Brown T, Stoyanova R. *Conf Proc IEEE Eng Med Biol Soc* 2005;2:1095-1098.